Audio Engineering Society

Convention Paper 9915

Presented at the 144th Convention
2018 May 23–26, Milan, Italy

This Convention paper was selected based on a submitted abstract and 750-word precis that have been peer reviewed by at least two qualified anonymous reviewers. The complete manuscript was not peer reviewed. This convention paper has been reproduced from the author's advance manuscript without editing, corrections, or consideration by the Review Board. The AES takes no responsibility for the contents. This paper is available in the AES E-Library, http://www.aes.org/e-lib. All rights reserved. Reproduction of this paper, or any portion thereof, is not permitted without direct permission from the Journal of the Audio Engineering Society.

Anti-Rattle System Loudspeaker Device

Dario Cinanni,[1] Carlo Sancisi[1]

[1]*ASK Industries Spa, subject to direction and coordination of JVCKENWOOD Corporation, via Dell'Industria, 12/14/16 - 60037 Monte San Vito (An) - Italy*

Correspondence should be addressed to Author (CinanniD@askgroup.it)

ABSTRACT

On the basis of loudspeaker cabinets and panels vibration problems, this paper deals with a new dynamic loudspeaker device capable to reduce mechanical vibrations transmitted to the panel where it is fixed. Virtual 3D prototype is designed and optimized by simulations. Simulations were carried out using analytical and finite element methods. A working prototype was realized, measured and then tested on a panel, in order to evaluate vibrations reduction.

1 Introduction

This paper deals with a solution based on an active anti-rattle system vibrating assembly generating an inertia force, moving coaxially and in phase opposition, with the loudspeaker moving assembly. The anti-rattle system vibrating assembly uses the loudspeaker's magnetic circuit and is constituted by a moving coil attached to a solid part and to a spring, integrated in the loudspeaker driver. The vibrating assembly study is based on the Tuned Mass Damper (TMD); starting on 2 Degree of Freedom TMD differential equation of motion, analytical solution of the ratio between mass and excursion is calculated and presented. Using masses and excursions analytical solutions, a new loudspeaker woofer 3D virtual prototype is arranged and the project is imported on the Multiphysics software in order to study interactions between loudspeaker driver and the anti-rattle system vibrating assembly. Magnetic assembly simulations are carried out optimizing pole plates sizes and also the spring element using Von Mises stress. Then a physical woofer prototype is implemented and measured in anechoic room. Acoustical measurements on IEC panel and on a closed box with the vibrating assembly ON and OFF are compared and the real electric impedance is matched with the simulated impedance. The woofer prototype is also mounted on a baffle, loaded with a Gaussian filtered noise on its terminals and a laser scanning vibrometer system is used to measure mechanical baffle oscillations due to vibrations transmitted by the transducer. Then displacement magnitude is displayed at different frequencies with anti-rattle system ON, in order to evaluate panel excursion reduction.

2 State of the art

One of the main design questions in loudspeaker enclosures concern vibrations reduction. An ideal cabinet would be infinitely rigid, so a section of an engineer work is focused on tend achieving this goal. Solutions depend by loudspeaker system audio field: Line Arrays, Automotive environments or hi-fi applications have different approaches to cabinets

design, due to context and layout constraints. Kinetic energy transmitted to panels by a loudspeaker driver is caused by acoustic radiation or mechanical transmission, particularly to:

- vibration from the air pressure variation in the cabinet (sound pressure inside the cabinet is generated from the rear loudspeaker membrane and it is in anti-phase compared to front membrane radiation; the sound transmitted by the panels where loudspeaker driver is fixed interferes with that from the membrane causing irregularities in both the steady-state axial frequency response curve and in the polar diagram);
- vibration through the reactive force from the loudspeaker unit (loudspeaker moving assembly mass oscillations are transferred to panels through the basket by mechanical transmission);
- vibration from movement of other panels (it happens widely in automotive environments).

Several studies on both sound pressure inside the cabinet and mechanical resonances have been conducted, demonstrating how cabinet vibrations -if not controlled- could influence negatively sound reproduction. Starting by old studies on acoustical resonances and panel enclosure vibrations by Iverson [1], Backman [2] [3], Lipshitz et al. [4], Stevens [5], Døssing et al. [6], Tappan [7], recent examples using modern tools have been done by Karjalainen et al. [8], Bastyr and Capone [9], Cobianchi and Rousseau [10] using BEM/FEM and laser Doppler measurement or Demoli and Djurek [11] used a timeaveraged digital holographic technique by hot wire anemometry and laser interferometry.

Automotive OEM is one of the worst application field for structural resonances influencing sound reproduction, increasingly demanding lightweight for used box materials, and moreover for environment coupling parts are an easy way for structural vibrations generated by low inertia low frequency loudspeakers. Studies about doors rattle and vibration noise generated by other parts inside a car have been done by many car makers, Nakashima et al. [12], Hsieh et al. [13], Narayana [14] are some interesting examples.

Generally remedial treatments used to reducing resonances problems caused by baffle vibrations are bracing, damping and/or density increasing of vibrating panels. Several studies about this topic (how to improve cabinet performances) have been conducted, one of the last examples is Nyholm et al. [15]. On inventions field, ingenious patented solutions are related to:

- Active damping with drivers mounted in a “back to back” compound configuration (for example Bose [16] [17] [18] and Kef [19]), using also passive radiators (for example Matsushita Electric Industrial [20] and Bose [21]);
- Active damping with masses (for example Sony [22], Hikida [23] and ASK [24]);
- Passive damping with masses (for example Genelec [25] and Fujitsu Ten [26]) or decoupling air volume of the loudspeaker rear emission (for example B&W [27]).
- Mutual induction (for example Huayn Electronics [28])

The first point involves both mechanical and acoustic, the others mechanical interactions only.

3 Standard model setup

Firstly, a standard woofer was implemented, using a ordinary ferrite magnetic assembly, steel basket, rubber surround and a paper cone. Parts are visible in fig. 1.

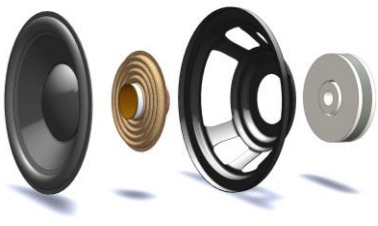

Figure 1. Exploded loudspeaker parts.

Then the same loudspeaker 3D design was imported in the Multiphysics software, solved for the magnetic field and structural mechanics physics. Tuning the simulated driver behavior the aim was to obtain a working virtual prototype useful to arrange different solutions for the purpose to reduce mechanical vibrations. The first diagram to analyze in a mechanical system is the electric impedance analyses. Particular attention is paid to the resonance frequency and the resonance peak entity. Considering that, the only assumption used to simplify the model is that exit wire leads are not modelled.

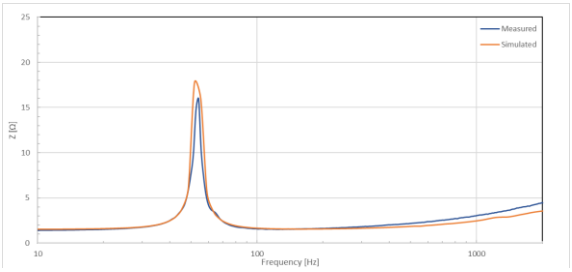

Figure 2. Loudspeaker electric impedance, measurement vs simulation plot comparison.

The exit wire leads increasing total direct current resistance, weren't modelled as 3D design, but were included in the model anyway. Gravity forces are applied to all domains and gravity node acts in the negative direction parallel to the axis loudspeaker membrane movement.
Then the real loudspeaker prototype moving parts were measured using a laser placed on membrane center along its axis movement. See fig. 3.

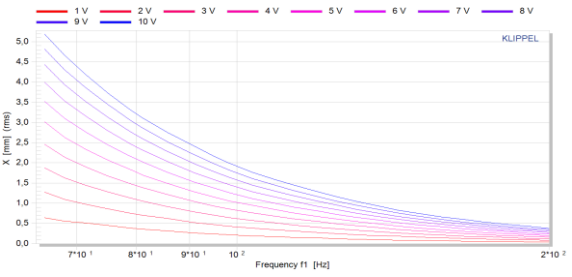

Figure 3. RMS displacement vs frequency and amplitude.

The transducer was loaded with different amplitudes, to understand nonlinear mechanism entity when out of small signal domain.

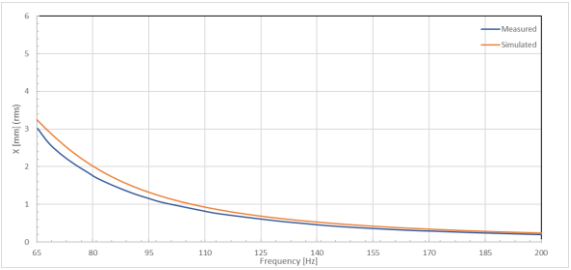

Figure 4. RMS displacement vs frequency @5V amplitude. Measurement vs simulation plot comparison.

Then the displacement plot measured @5V is used to compare if amplitude compression values match the simulated model at high signal amplitude. See fig. 4.
Displacement graph also suggests to consider 1kHz as the maximum frequency for the vibration analysis.

4 Driver magnetic study

Static magnetic study is necessary to complete all information useful to find a solution on how to implement an Anti-Rattle system on the transducer using the same motor.

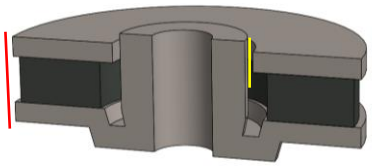

Figure 5. Transducer magnetic assembly and cut lines displayed for flux density analysis.

Considering the transducer magnetic assembly in fig. 5, the result of magnetic flux density along the cut line inside magnetic gap is given by fig. 6. Considering the transducer magnetic assembly in

fig. 5, the result of magnetic flux density along the cut line on the magnetic assembly external side is given by fig. 7.

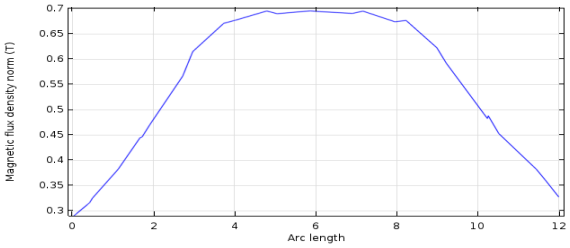

Figure 6. Magnetic flux density plotted on the cut line inside transducer gap.

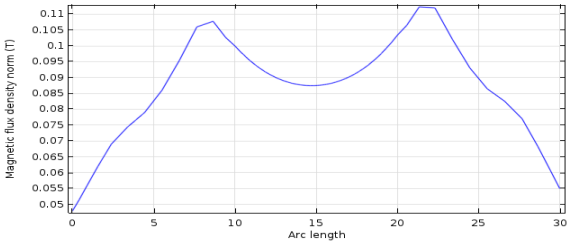

Figure 7. Magnetic flux density plotted on the cut line on the magnetic assembly external side.

This graph represents the magnetic flux line path on external perimeter around the loudspeaker pole plates, at 15mm arc length there is the magnet center. Magnetic flux is very low because of distance between the two plates. And the two peaks are not symmetric because of the steel amount in the two pole plates. It's possible to use this area as a base for a motor structure for the vibration damper.
Now the virtual prototype is ready to study how sizing the damper.

5 Tuned Mass Damper

An Anti-Rattle structure attached to a loudspeaker in a mechanical system can be identified as a dynamic response damper. This structure is commonly referred to a TMD (Tuned Mass Damper) with 2-DOF (2 degree of freedom) [29].
Generally the TMD frequency is tuned to a particular structural frequency of an oscillator (Loudspeaker), so that when that frequency is excited, the second oscillator (Anti-Rattle) will resonate out of phase with the structural motion. In fig. 3 is shown a 2DOF TMD, where M, K, C represent respectively loudspeaker mass, stiffness and damping, whereas m, k, c represent respectively anti-Rattle mass, stiffness and damping.

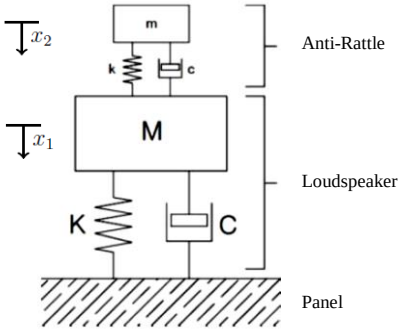

Figure 8. 2DOF TMD.

x1, x2 represent respectively absolute positions of M and m and frequently the relative position of m compared to M is used, assuming x2-x1 instead x2. With a 2-DOF system is possible to work on the vibration noise source (loudspeaker), but in some cases the system became more complex with N degree of freedom. For example, automotive environment are full of vibrating parts that could vibrate also for acoustic pressure. In this case is possible to use an AFTMD (Active Feedback Tuned Mass Damper) controlling TMD with a DSP (Digital Sound Processor) through a sensors feedback. Displacement amplitude for a classic TMD sizing is usually oriented to some orders of magnitude more than displacement of M, because TMD are used for damping seismic events or wavy wind pressure on buildings.
Assuming that the damping force is proportional to velocity and there is a periodic force $p0\ cos(\omega t)$ applied on M, simplifying with C= 0, it is possible to get the following differential equations as the motion system expression

$$Mx1" + Kx1 + k(x1 - x2) + c(x1' - x2') = p0\ cos(\omega t)$$

$$mx2" + k(x2 - x1) + c(x2' - x1') = 0$$

Where x1' is the time derivative of x1. Replacing the first equation by the sum of the two equations gives

$$Mx1" + Kx1 + mx2" = p0\,cos(\omega t)$$

$$mx2" + k(x2 - x1) + c(x2' - x1') = 0$$

Finding periodic solutions as
$x1 = a\cos(\omega t) + b\,sen(\omega t)$
$x2 = c\cos(\omega t) + d\,sen(\omega t)$

Substituting periodic solutions into the differential equations gives the following algebraic system of equations.

$$\begin{pmatrix} K - M\omega^2 & 0 & -m\omega^2 & 0 \\ 0 & K - M\omega^2 & 0 & -m\omega^2 \\ -k & -c\omega & k - m\omega^2 & c\omega \\ c\omega & -k & -c\omega & k - m\omega^2 \end{pmatrix} \begin{pmatrix} a \\ b \\ c \\ d \end{pmatrix} = \begin{pmatrix} p0 \\ 0 \\ 0 \\ 0 \end{pmatrix}$$

Call the coefficient matrix **M**, it is possible to write and invert **M** in a block form

$$\mathbf{W} = \begin{pmatrix} 0 & 1 \\ -1 & 0 \end{pmatrix},\ \mathbf{M} = \begin{pmatrix} A & B \\ C & D \end{pmatrix},$$

where
*A= r1I, B = r2I, C = r3I - s1**W**, D = r4I + s1**W**,*
$r1 = K - M\omega^2$, $r2 = -m\omega^2$, *r3 = -k*, $r4 = k - m\omega^2$, $s1 = c\omega$

Commutating A and B

$$\mathbf{M^{-1}} = \begin{pmatrix} (AD - BC)^{-1} & 0 \\ 0 & (AD - BC)^{-1} \end{pmatrix} \begin{pmatrix} D & -B \\ -C & A \end{pmatrix}$$

Defining *r* and *s as*
*AD - BC = (r1r4 - r2r3)I + s1(r1 + r2)**W** = rI + s**W***

So that
$$(AD - BC)^{-1} = \frac{1}{r^2 + s^2}(rI - s\boldsymbol{W})$$

and
$$\begin{pmatrix} a \\ b \\ c \\ d \end{pmatrix} = \frac{p0}{r^2 + s^2} \begin{pmatrix} \mathrm{rr4} + \mathrm{ss1} \\ -\mathrm{rs1} + \mathrm{sr4} \\ -\mathrm{rr3} + \mathrm{ss1} \\ -\mathrm{rs1} - \mathrm{sr3} \end{pmatrix}$$

x1 amplitude is A1= $\sqrt{a^2 + b^2}$ and x2 amplitude is A2= $\sqrt{c^2 + d^2}$

obtaining

$$A1 = \frac{p0}{r^2 + s^2}(r4^2 + s1^2)$$
$$A2 = \frac{p0}{r^2 + s^2}(r3^2 + s1^2)$$

Explicating parameters it is possible to write $A1^2$ and $A2^2$

$$A1^2 = p0^2 \frac{c^2\omega^2 + (k - m\omega^2)^2}{[(K - M\omega^2)(k - m\omega^2) - (k - m\omega^2)]^2 + c^2\omega^2 + (K - M\omega^2 - m\omega^2)^2}$$

$$A2^2 = p0^2 \frac{c^2\omega^2 + k^2}{[(K - M\omega^2)(k - m\omega^2) - (k - m\omega^2)]^2 + c^2\omega^2 + (K - M\omega^2 - m\omega^2)^2}$$

Writing standard constants
Eigenfrequencies: $\omega 1^2 = \frac{K}{M}$ $\omega 2^2 = \frac{k}{m}$
Mass ratio: $\mu = \frac{m}{M}$

The higher the mass of the TMD the better the damping is. Commonly ranges are from 0.02 (often low effect) up to 0.1 (often a constructive limit in standard applications).

Damping ratio: $\xi_2 = \frac{c}{2m\,\omega 2^2}$
obtaining from the damping ratio
$c = 2\,\xi_2 m\,\omega 2^2$
$C = 2\,\xi_1 m\,\omega$

Stiffness relation: $k = \mu\,K$
The best efficiency for the frequency of damper is given at the structure fundamental frequency
$\omega 2 = \omega 1$
$f = \frac{\omega 2}{\omega 1}$

Optimal frequency is
$\omega 2 = f_{opt}\,\omega 1$

Considering periodic excitation
$p = p0\,sen(\Omega t)$

$u1 = x1\,sen(\Omega t + \delta 1)$
$u2 = x2\,sen(\Omega t + \delta 1 + \delta 2)$

where x e δ represent respectively amplitude and phase of the displacement. Critical load is given by resonance condition $\Omega = \omega$, in this case in the form

$$x1 = \frac{p0}{K\mu}\sqrt{\frac{1}{1+\left(\frac{2\xi_1}{\mu}+\frac{1}{2\xi_2}\right)^2}} \quad (1)$$

$$x2 = \frac{1}{2\xi_2}x1 \quad (2)$$

$$tan\,\delta1 = \left[\frac{2\xi_1}{M}+\frac{1}{2\xi_2}\right]$$

$$tan\,\delta2 = -\frac{\pi}{2}$$

TMD mass response is 90° out of phase compared to primary mass. This phase difference produces dissipation energy given by inertia force of the damper. Without damper the response is given by

$$x1 = \frac{p0}{K}\left(\frac{1}{2\xi_1}\right)$$

$$\delta1 = -\frac{\pi}{2}$$

expressing (1) to compare these two cases in terms of equivalent damping ratio

$$x1 = \frac{p0}{K}\left(\frac{1}{2\xi_e}\right)$$

where

$$\xi_e = \frac{\mu}{2}\sqrt{1+\left(\frac{2\xi_1}{M}+\frac{1}{2\xi_2}\right)^2} \quad (3)$$

(3) represents damper parameter contribution to the total damping. Increasing the mass ratio, the damping will increase. Reducing TMD damping coefficient, the total damping will increase. (2) gives a limit to the damper relative displacement.

6 Anti-Rattle loudspeaker system design

Adding two plane springs, a magnetic metal cylinder and a two windings voice coil in the same loudspeaker in fig. 1 we obtain an active oscillator system moving coaxially to the loudspeaker membrane in fig. 2 [30]. It is possible to excite the oscillator voice coil with 3 types of signals:

1) in phase opposition compared to loudspeaker voice coil (in this case the structure has an Anti-Rattle function);
2) in phase compared to loudspeaker voice coil (in this case the structure has a Bass Enhancer function);
3) in both phase/antiphase compared to loudspeaker voice coil, using a DSP (in this case the structure function could became an equalizer of mechanical vibrations/acoustic pressure emission).

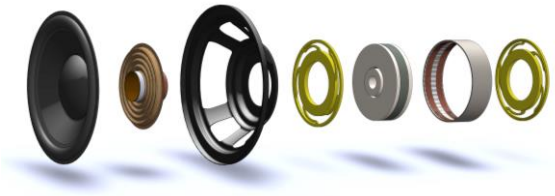

Figure 9. Loudspeaker with the Anti-Rattle system.

Springs positions impose an axial movement to the oscillator, reducing unwanted movement but it is fundamental to simulate and study springs arms stress. See fig. 10. For the first sample the two springs are realized in a plastic polymer rapid prototyping. Related to current loudspeaker, Anti-Rattle excursion and mass will be dimensioned on the next chapter.

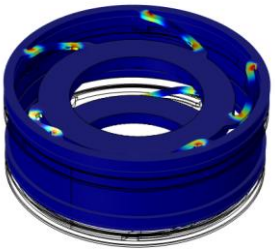

Figure 10. Von Mises Stress on Anti-Rattle springs.

7 Anti-Rattle system size

Assuming ξ = 0 and a damping factor of about 10%, considering $\xi_e = 0.1$ and using (3), the following relationship between μ e ξ_2 is obtained

$$\frac{\mu}{2}\sqrt{1+\left(\frac{2\xi_1}{M}+\frac{1}{2\xi_2}\right)^2}=0.1 \quad (4)$$

the relative displacement is obtained by (2), then combining (4), (2) and substituting $\xi = 0$

$$\frac{\mu}{2}\sqrt{1+\left(\frac{x2}{x1}\right)^2}=0.1 \quad (5)$$

approximating (5), removing radix and square terms,

$$\frac{\mu}{2}\left(\frac{x2}{x1}\right)\approx 0.1 \quad (6)$$

the general form of (6) following by (3) is

$$\mu \approx 2\xi_e\left(\frac{1}{\frac{x2}{x1}}\right)$$

and selecting for example $x2=\frac{x1}{20}$ an approximation of μ is

$$\mu=\frac{2\,(0.1)}{\frac{1}{20}}=4 \quad (7)$$

from (2)

$$\xi_2=\frac{1}{2}\left(\frac{x1}{x2}\right)=10$$

from stiffness proportion $k=\mu\,K$ getting $k=4K$

Taking a 10% damping, from (7) the Anti-Rattle mass has a ratio of 4:1 compared to the loudspeaker moving parts mass.

8 Anti-Rattle system magnetic study

The external metal cylinder in fig. 11 represents a new plate containing a new magnetic assembly and using the same loudspeaker motor.

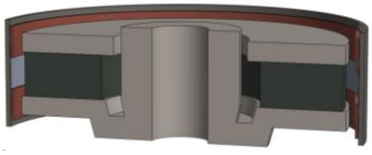

Figure 11. Loudspeaker with Anti-Rattle magnetic assembly side section.

The new magnetic assembly will create a double magnetic gap of fig. 12, in which the double windings Anti-Rattle voice coil will move.

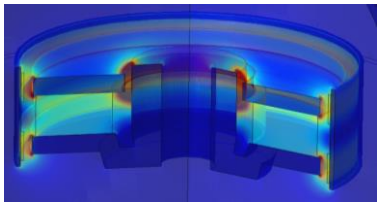

Figure 12. Magnetic flux in Loudspeaker and Anti-Rattle magnetic gaps.

Inside new magnetic gaps the induction flux of fig. 7 will be guided on a new path, becoming the plot in fig. 13.

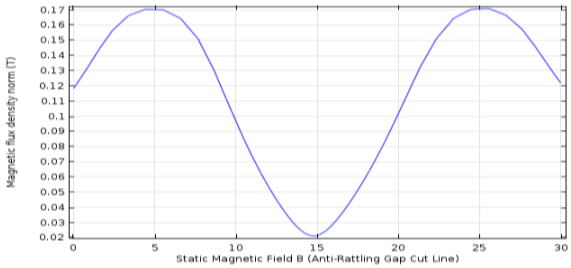

Figure 13. Magnetic flux density plotted inside the Anti-Rattle gaps. Same cut line of fig. 5.

Working on the whole magnetic circuit design now the two peaks are symmetric and absolute magnetic flux is increased, reducing of 0.1 T the total flux inside loudspeaker magnetic gap. See fig. 14.

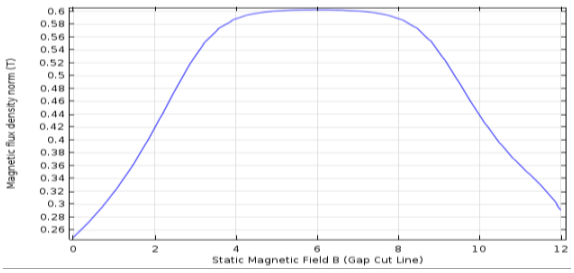

Figure 14. Magnetic flux density plotted on the cut line inside transducer gap. Same cut line of fig. 5.

The whole transducer is not optimized, but it represents a starting point for measurements and evaluations of the Anti-Rattle principle.

9 Anti-Rattle loudspeaker system measurement

A first measurement set has been done only to confirm that Anti-Rattle system has not a negative influence on loudspeaker behavior. Measurements were done in an anechoic room, initially transducer was mounted on IEC panel and loudspeaker was loaded with a sine sweep signal on its terminals. In fig. 15 the loudspeaker Total Harmonic Distortion (THD) plotted at 4W reveals a strange behavior in the range 50-80 Hz, in which the Anti-Rattle (in phase opposition compared to woofer) shows an increased THD behavior compared to the single loudspeaker.

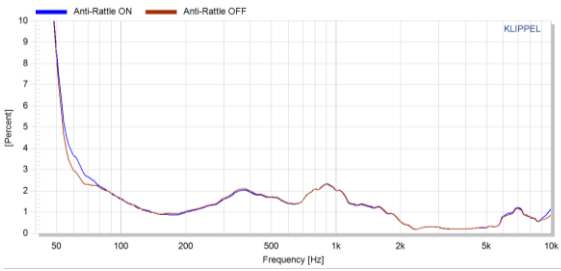

Figure 15. THD comparison of the Anti-Rattle system on/off @4W. Transducer mounted on IEC baffle.

Reversing the Anti-Rattle phase and plotting THD in fig. 16 the transducer behavior has changed in a way without correspondence to the measurement conducted before, as it is expected, because the frequency range is changed and the curve shape is not complementary to that of fig. 15.

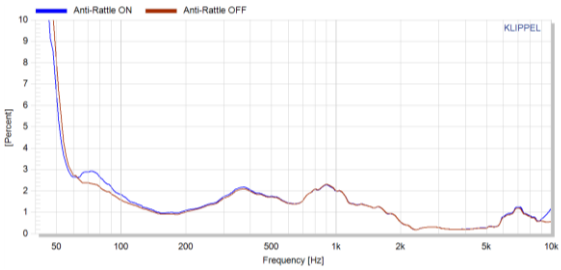

Figure 16. THD comparison of the Anti-Rattle system on/off @4W. Transducer mounted on IEC baffle. Anti-Rattle in phase with woofer.

Suspecting the problem is due to transducer fixing system and IEC panel, because of its great surface not perfectly rigid and fixed in some points creating non-harmonic vibration modes and acoustic cancelations on microphone. A second measurement set has been done. All first measurement set were repeated with the loudspeaker mounted on a closed box. Some variables were eliminated, building a closed box with high mass panels that for a 4W measurement it's possible to consider the transducer mounted on an infinitely rigid panel. Hence comparing fig. 17 to fig. 18 it's possible to see the complementary transducer THD behavior in the range 100÷500 Hz. Increasing the input power this difference will increase.

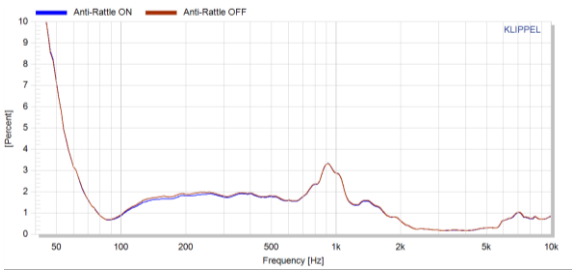

Figure 17. THD comparison of the Anti-Rattle system on/off @4W. Transducer mounted in a closed box.

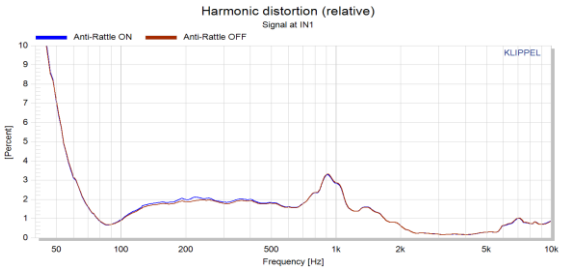

Figure 18. THD comparison of the Anti-Rattle system on/off @4W. Transducer mounted in a closed box. Anti-Rattle in phase with woofer.

THD difference in the frequency range 100÷500 Hz is independent on panel vibrations but is related to loudspeaker structure itself. Consequently, fig. 17 plot demonstrates a THD reduction of the loudspeaker with Anti-Rattle system ON. This reduction is not due to panel movement but to the

loudspeaker structural vibration modes. It's possible to arrive to this conclusion using an eigenfrequencies simulation shown in fig. 19, this is the structure vibration mode excited by loudspeaker moving parts and controlled by Anti-Rattle oscillations.

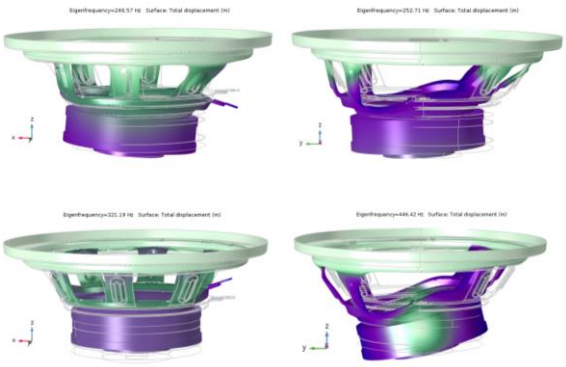

Figure 19. Excited Eigenfrequencies. Transducer with fixed constraints on basket screws.

Eigenfrequencies analysis indicates that first 4 modes are in the range 246÷446 Hz. Giving the Eigenfrequency mode vector of movement, in which Anti-Rattle system has a great impact on loudspeaker structure, the third mode at 321 Hz is the most excited frequency. Another measurement that has been done is shown in fig. 20. This measurement represents the amplitude and modulation distortion in which the plot of the loudspeaker only is compared to the same loudspeaker with the Anti-Rattle system turned on.

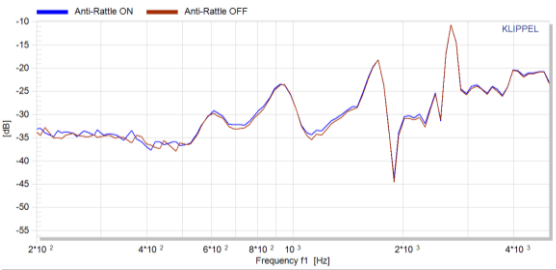

Figure 20. Amplitude and modulation distortion comparison of the Anti-Rattle system on/off. Transducer mounted in a closed box.

The frequency response, of the transducer mounted in a closed box, is shown in fig. 21 and it is obtained in anechoic room at 1m distance by the microphone, on loudspeaker axis, applying 4W power.

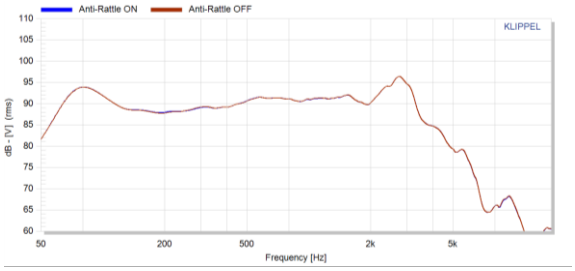

Figure 21. Frequency response comparison of the Anti-Rattle system on/off @4W. Transducer mounted in a closed box.

Taking into account fig. 17, fig. 20 and fig. 21, a first conclusion is that Anti-Rattle system cannot damage loudspeaker acoustic performances, at least it helps loudspeaker eliminating structure self-vibrations. Next step is the panel vibration reduction evaluation, for this purpose the transducer is mounted on a wooden flat panel 400x400mm, 8mm thickness. Using a laser scanner vibrometer a structural Frequency Response Function (FRF) measurement has been done and plotted in fig. 22.

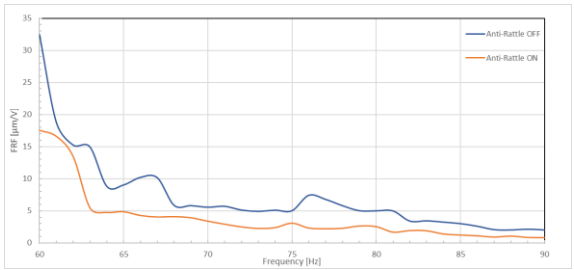

Figure 22. FRF comparison of the Anti-Rattle system on/off of a wooden panel, with transducer mounted on and exited by a filtered Gaussian Noise.

To obtain the structural FRF, a Gaussian White Noise, filtered in the range 60-90 Hz, is used to excite loudspeaker and the panel. FRF is useful to quantify the structural transfer between the loudspeaker and the panel. This last measurement is

useful to understand that the principle is valid, and the system works in the proper manner. It doesn't have to be considered in absolute value, it's indicative only because it depends by the point on the panel surface in which is measured.

10 Conclusions

Anti-Rattle system doesn't represent a loss factor for loudspeaker acoustic performances. On the contrary it helps loudspeaker eliminating structure self-vibrations. The first developed prototype reveals about 50% of panel vibrations reduction.
Future extension of this study will be made to use a more efficient driver with a hypothetical anti-Rattle system designed for a production line. Then the simulated model could be extended adding acoustic interactions (FEM or BEM) to investigate and correct panel vibrations due to acoustic pressure. Furthermore, the development of a DSP to tune Anti-Rattle phase to meet real environment needs will then be attempted.

11 Acknowledgements and used tools

The author wishes to acknowledge the assistance of Dr. A. Lapi for his support on laser scanning measurements.
Used tools: *Solidworks* for 3D design, *Comsol Multiphysics* for simulations, *Virtual Voice Coil* for voice coils calculations, *Klippel system* for anechoic measurement, *Laser Scanner Vibrometer* developed by ASK.

References

[1] J. K. Iverson, *The Theory of Loudspeaker Cabinet Resonances*, AES 42nd Convention, Los Angeles, California, 1972 May 5.

[2] J. Backman, *Effect of Panel Damping on Loudspeaker Enclosure Vibration,* AES 101st Convention, Los Angeles, California, 1996 November 8–11.

[3] J. Backman, *Computing the Mechanical and Acoustical Resonances in a Loudspeaker Enclosure,* AES 102nd Convention, Munich, Germany, 1997 March 22-25.

[4] S. Lipshitz, M. K. Heal, J. Vanderkooy, *An Investigation of Sound Radiation by Loudspeaker Cabinets,* AES 90th Convention, Paris, France, 1991 February 19-22.

[5] S. W. Stevens, *Sound Radiated from loudspeaker Cabinets,* AES 50th Convention, London, UK, 1975 March.

[6] O. Døssing, C. Hoffmann, L. Matthiessen, O. J. Veiergang, *Measurement of Operating Modes on a Loudspeaker Cabinet,* AES 87th Convention, New York, US, 1989 October 18-21.

[7] P. W. Tappan, *Loudspeaker Enclosure Walls,* J. Audio Eng. Soc., Vol. 10, No. 3, 1962 July.

[8] M. Karjalainen, V. Ikonen, P. Antsalo, P. Maijala, L. Savioja, A. Suutala, S. Pohjolainen, *Comparison of Numerical Simulation Models and Measured Low-Frequency Behavior of Loudspeaker Enclosures,* J. Audio Eng. Soc., Vol. 49, No. 12, 2001 December.

[9] K. J. Bastyr, D. E. Capone, *On the Acoustic Radiation from a Loudspeaker's Cabinet,* J. Audio Eng. Soc., Vol. 51, No. 4, 2003 April.

[10] M. Cobianchi, M. Rousseau, *Predicting the Acoustic Power Radiation from Loudspeaker Cabinets: a Numerically Efficient Approach,* AES 139th Convention, New York, US, 2015 October 29 - November 1.

[11] N. Demoli, D. Djurek, *Vibrations in the loudspeaker enclosure evaluated by hot wire anemometry and laser interferometry,* AES 130th Convention, London, UK, 2011 May 13-16.

[12] M. Nakashima, Y. Hamada, A. Van Gils, I. Bosmans, C. Coster, D. Sacré, *Experimental and numerical analysis of loudspeaker induced door rattle*, Proceedings of ISMA 2016.

[13] S. R. Hsieh, V. J. Borowski, J. Y. Her, S. W. Shaw, *A CAE Methodology for Reducing Rattle in Structural Components*, SAE Technical Paper, 1502, 1997.

[14] N. Narayana, *A Finite Element Method for Effective Reduction of Speaker-Borne Squeak and Rattle Noise in Automotive Doors*, SAE Technical Paper, 1583, 2011.

[15] H. B. J. Nyholm, J. C. Severinsen, H. Schneider, N. H. Mortensen, M. A. E. Andersen, *Construction of Lightweight Loudspeaker Enclosures,* AES 142nd Convention, Berlin, Germany, 2017 May 20-23.

[16] K. J. Bastyr, C. B. Ickler, R. S. Wakeland, *System and Method for Reduced Baffle Vibration,* US patent 2009/0257611, 2009 October 15.

[17] K. J. Bastyr, M. W. Stark, *System and Method for Reducing Baffle Vibration,* US patent 2010/0027816, 2010 February 4.

[18] G. Nichols, M. D. Rosen, H. P. Greenberger, *Baffle Vibration Reducing,* US patent 7,983,436, 2011 July 19.

[19] M. A. Dodd, *Loudspeaker with Force Cancelling Configuration,* US patent 9,191,747, 2015 November 17.

[20] S. Tanaka, K. Tamura, S. Kageyama, *Bass Speaker,* US patent 5,850,460, 1998 December 15.

[21] G. C. Chick, H. P. Greenberger, R. Litovsky, C. B. Ickler, R. Mark, G. Nochols, *Passive Acoustic Radiating,* US patent 7,133,533, 2006 November 7.

[22] S. Egawa, K. Inanaga, K. Maeda, A. Shimizu, *Deleterious Mechanical Vibrations from Dynamic Loudspeaker Offset by Additional Dynamic Device,* US patent 4,176,249, 1979 November 27.

[23] T. Hikida, *Speaker Balancer,* JP patent 2218298, August 08 1990.

[24] M. Servadio, *Electro-Magnetic Transducer and Vibration Control System,* US patent 2015/0280634, 2015 October 1.

[25] A. Mäkivirta, A. Varla, *Method and Arrangement for attenuating Mechanical Resonance in a Loudspeaker,* EP patent 0917396, 1998 November 11.

[26] H. Kowaky, A. Nichikawa, K. Tsumori, H. Yoshii, *Speaker Apparatus,* EP patent 1206162, 2001 September 11.

[27] S. T. Nevill, *Decoupled Drive Unit for a Loudspeaker Enclosure,* US patent 9,241,206, 2016 January 19.

[28] G. Zhao, B. Zhu, *Loudspeaker,* CN patent 204031441, 2014 August 07.

[29] F. Cheli, G. Diana, *Dinamica e Vibrazione dei Sistemi,* Utet Libreria, Reprint 1997.

[30] D. Cinanni, A. Falcioni, C. Sancisi, *Altoparlante con Sistema di Controllo delle Vibrazioni,* patent pending.